

1 **Ecological examples of nonstationarity, nonlinearity, and statistical**
2 **interactions in dynamic structural equation models**

3

4 Running header: nonlinear and nonstationary structural equations

5

6 James T. Thorson^{1*}, Kasper Kristensen²

7

8 ¹ Resource Ecology and Fisheries Management Division, Alaska Fisheries Science Center,
9 National Marine Fisheries Service

10 ² Technical University of Denmark, Lyngby, Denmark

11 * Corresponding author: James.Thorson@noaa.gov

12

13 **Authorship statement**

14 J. Thorson developed code in *dsem*, and K. Kristensen modified TMB to enable efficient
15 estimation. J. Thorson led analysis, data curation, and writing, and both authors contributed to
16 editing.

17

18 **Acknowledgements**

19 We thank Steve Munch for providing the copy of Didinium-Paramesium abundance, Mahaffy
20 (2009) for the digitized copy of Hare-Lynx abundance used here, Daniel Schindler for curating
21 the Lake Washington sampling data, and the MARSS developers (Eli Holmes, Eric Ward, and
22 Mark Scheuerell) for distributing the Lake Washington sampling data in easy-to-use format. We
23 also thank Grant Adams and Jennifer Bigman for helpful comments on an earlier draft.

24

25 **Data accessibility and reproducibility**

26 Data for sea surface temperature at Departure Bay are available online:

27 <https://open.canada.ca/data/en/dataset/719955f2-bf8e-44f7-bc26->

28 [6bd623e82884/resource/17c30115-25de-4bad-9286-51d3ef467793](https://open.canada.ca/data/en/resource/17c30115-25de-4bad-9286-51d3ef467793), and we use the copy from

29 July 23, 2025 and downloaded Nov. 3, 2025. Data for the Pacific Decadal Oscillation were

30 downloaded from JISAO (<http://research.jisao.washington.edu/pdo/PDO.latest.txt>) on Nov. 6,

31 2018, as analyzed previously by Thorson et al. (2020). Data for Lake Washington are from the

32 MARSS package release 3.11.9 (Holmes et al., 2012), as collected by Dr. W. T. Edmondson,

33 funded by the Andrew Mellon Foundation, and curated by Dr. Daniel Schindler.

34 All analysis is conducted using R-package *dsem* release 2.0.0 ([https://github.com/James-](https://github.com/James-Thorson-NOAA/dsem@dev)

35 [Thorson-NOAA/dsem@dev](https://github.com/James-Thorson-NOAA/dsem@dev)). Code and data to reproduce all figures is available in a GitHub

36 repo (<https://github.com/James-Thorson/DSEM-varying-paths>), publicly available upon

37 acceptance and distributed as a ZIP file during peer review.

38

39

40 **Abstract:**

41 1. Ecologists are adapting structural causal modelling for spatial, phylogenetic, and time-series
42 analysis. However, ecological extensions of path analysis and structural equation models
43 (SEM) typically assume that interactions (“path coefficients”) are stationary, linear, and
44 additive, while ecological and evolutionary dynamics are often nonstationary, nonlinear, and
45 include statistical interactions.

46 2. Here, we combine moderated SEM (estimating path coefficients as model variables) with
47 dynamic SEM (estimating both simultaneous and lagged interactions among variables),
48 develop a new “path-lag-slope” notation to specify this combination, and demonstrate it
49 using a simulation experiment and three ecological case studies.

50 3. The simulation experiment confirms that an autocorrelated “random-slope” model can
51 estimate the nonstationary impact of one variable on another, but that the random slope is
52 shrunk towards a constant value as data become less informative. The first case study then
53 demonstrates nonstationarity by estimating an autoregressive slope linking a regional climate
54 index to local ocean temperature near Vancouver Island. The second demonstrates
55 nonlinearity by approximating Lotka-Volterra dynamics for two predator-prey systems,
56 which closely match estimates of interactions and carrying capacity from traditional
57 ordinary-differential equation methods. The third demonstrates statistical interactions by
58 using monthly plankton samples (1962-1994) to show that resource-consumer-predator
59 interactions in Lake Washington have a dome-shaped response to temperature.

60 4. We envision several uses in causal analysis: (1) testing whether path coefficients are
61 nonstationary; (2) estimating nonlinear responses given missing data; and (3) linking
62 ecological parameters to hypothesized drivers in applied modelling.

63

64 Keywords: Dynamic structural equation model; random slopes; moderated structural equation
65 model; nonstationary; Lotka-Volterra model

66

67 **Introduction**

68 Ecologists are showing an increasing interest in causal analysis (Arif & MacNeil, 2022;
69 Byrnes & Dee, 2025; Grace, 2024; Larsen et al., 2019). Ecological applications of causal
70 analysis have typically used path analysis (PA) or structural equation models (SEM) to identify
71 direct and indirect consequences of hypothetical policy or environmental changes. These models
72 require hypothesizing linear structural relationships among a set of variables (e.g., *A* causes *B*
73 and *B* causes *C*), where the strength of relationships is then estimated from the covariance of
74 samples. The fitted model can be used to identify how a policy changing one variable results in
75 direct and indirect effects on other model variables (in the previous example, for example, a
76 change in *B* would affect *C* but not *A*, despite all variables being correlated).

77 In particular, ecologists are adapting SEM and PA for ecological contexts such phylogenetic,
78 spatial, and time-series analysis. For example, evolutionary ecologists are using phylogenetic
79 structural equation models (PSEM) or path analysis (PPA) to identify evolutionary relationships
80 among species traits (Thorson et al., 2023; von Hardenberg & Gonzalez-Voyer, 2013). Similarly,
81 community ecologists are developing spatial extensions of SEM to estimate species interactions
82 that underlie observed covariance in densities among species across sites (Papadogeorgou et al.,
83 2023; Thorson et al., 2025). Finally, population ecologists are extending prior developments in
84 multivariate autoregressive (MAR) models (Ives et al., 2003; Wootton & Emmerson, 2005) to
85 develop dynamic structural equation models (DSEM), which estimates both simultaneous and
86 lagged interactions using ecological time-series (Thorson et al., 2024), based on similar models
87 in psychology (Asparouhov et al., 2018).

88 Despite this growing interests, SEM and PA typically require assuming that ecological
89 relationships are stationary, linear, and additive. These assumptions conflict with the general

90 recognition that many parameters of ecological models vary across time, space, and phylogenies
91 (Ives, 2022; Rollinson et al., 2021), that ecological relationships (e.g., metabolic response to
92 temperature) are nonlinear (Munch et al., 2018), and that species interactions might be context-
93 dependent such that regression models should include statistical interactions (Hixon & Carr,
94 1997). Existing extensions of SEM and PA can account for nonstationarity, nonlinearity, and
95 statistical interactions in some special cases. For example, when causal relationships are
96 unidirectional and data are free of missing values, ecologists can use generalized additive models
97 within “piecewise SEM” (Lefcheck, 2016) to estimate nonlinear linkages. Similarly, SEM (and
98 its spatial, temporal, and phylogenetic extensions) can incorporate latent variables to identify
99 some forms of nonstationarity (i.e., random covariation in average densities among sites).

100 Alternatively, SEM can be extended to incorporate “moderated” interactions, e.g., where the
101 effect of covariate X on response Y depends upon a moderating variable W (i.e., $\mathbb{E}(Y) = \beta_X X +$
102 $\beta_{XW} XW$). The moderated variable W might be observed (such that XW is included as covariate
103 to represent the statistical interaction of X and W) or unobserved (such that $\beta_{XW} W$ is treated as a
104 random-slope for covariate X). In either case, a “moderated-SEM” (MSEM) can be applied to
105 correct for the statistical interaction or nonstationary slope parameter. However, MSEM was not
106 discussed in recent ecological reviews for causal modelling (Arif & MacNeil, 2022; Byrnes &
107 Dee, 2025; Grace, 2024; Larsen et al., 2019), and has seen limited use in ecological modelling
108 (although see Papadogeorgou et al., 2023)

109 In this study, we demonstrate how SEM can be extended to estimate nonstationary
110 parameters, nonlinear relationships, and statistical interactions. We specifically combine DSEM
111 (which handles missing data as well as simultaneous and lagged relationships among variables)
112 with MSEM (which estimates nonstationarity, nonlinearity, and statistical interactions). We also

113 introduce a novel “path-lag-slope” notation for specifying moderated DSEM (“MDSEM”)
114 available within the R-package *dsem* version 2.0.0. Finally, we demonstrate the model and
115 software using three varied examples. We specifically address (1) *nonstationarity* using a
116 varying-slopes model for the relationship between temperature and regional climate; (2)
117 *nonlinearity* using a SEM implementation of species interactions using the Lotka-Volterra
118 equations; and (3) and *statistical interactions* using a resource-consumer-predator model
119 involving species interactions that have a dome-shaped response to temperature.

120 Methods

121 We seek to extend dynamic structural equation models to include nonstationarity, nonlinearity,
122 and statistical interactions. To do so, we adapt moderated SEM (MSEM) for use in the Gaussian
123 Markov random field (GMRF) that is used when estimating dynamic SEM (DSEM). We start by
124 reviewing this GMRF implementation of DSEM.

125 DSEM describes the relationship among $j \in \{1, 2, \dots, J\}$ variables over $t \in \{1, 2, \dots, T\}$ time-
126 intervals, assembled in a matrix \mathbf{X} with dimension $T \times J$ containing values x_{tj} for each time and
127 variable. It is then fitted using a $T \times J$ matrix \mathbf{Y} containing measurements y_{tj} (where y_{tj} might
128 also include missing values that are specified as NA). We define operator $\text{vec}(\mathbf{X})$ as stacking the
129 columns of \mathbf{X} into a single vector with length TJ , and \mathbf{x}_t as the J length row-vector containing x_{tj}
130 for all variables in time t . DSEM also specifies that variables have unmodeled sources of
131 variation which result in exogenous variation \mathbf{E} with dimension $T \times J$, where $\text{vec}(\mathbf{E})$ again stacks
132 columns into a single vector, and $\mathbf{\epsilon}_t$ is the error in year t . DSEM then defines a vector-
133 autoregressive process for \mathbf{x}_t :

134
$$\mathbf{x}_t = \underbrace{\mathbf{B}_0 \mathbf{x}_t}_{\text{Simultaneous}} + \underbrace{\mathbf{B}_1 \mathbf{x}_{t-1}}_{\text{Lag-1}} + \underbrace{\mathbf{B}_2 \mathbf{x}_{t-2}}_{\text{Lag-2}} + \dots + \underbrace{\mathbf{B}_k \mathbf{x}_{t-k}}_{\text{Higher-order}} + \mathbf{\epsilon}_t$$

135 where \mathbf{B}_0 are simultaneous interactions among variables, \mathbf{B}_1 and \mathbf{B}_2 are lag-1 and lag-2
 136 interactions, and the model can include any arbitrary lag up to $T - 1$. This vector-autoregressive
 137 notation is then rewritten as a joint simultaneous equation model (SEM), while assembling the
 138 lag matrices ($\mathbf{B}_0, \mathbf{B}_1, \mathbf{B}_2, \dots$) in a joint path matrix $\mathbf{P}_{\text{joint}}$ with dimensions $TJ \times TJ$:

$$\text{vec}(\mathbf{X}) = \mathbf{P}_{\text{joint}} \text{vec}(\mathbf{X}) + \text{vec}(\mathbf{E}) \quad (1)$$

$$\text{vec}(\mathbf{E}) \sim \text{MVN}(\mathbf{0}, \mathbf{V}_{\text{joint}})$$

139 where $\text{vec}(\mathbf{E})$ has variance $\mathbf{V}_{\text{joint}}$ with dimension $TJ \times TJ$. Algebra then shows that:

$$\text{vec}(\mathbf{X}) \sim \text{GMRF}(\mathbf{0}, \mathbf{Q}) \quad (2)$$

$$\mathbf{Q} = (\mathbf{I} - \mathbf{P}_{\text{joint}}^T) \mathbf{V}_{\text{joint}}^{-1} (\mathbf{I} - \mathbf{P}_{\text{joint}})$$

140 where the probability density for this GMRF can be efficiently evaluated to estimate values for
 141 $\mathbf{P}_{\text{joint}}$.

142 To allow users to specify what combination of simultaneous and lagged effects are estimated
 143 (i.e., the non-zero elements of lag-matrices lag matrices $\mathbf{B}_0, \mathbf{B}_1, \mathbf{B}_2, \dots$), DSEM introduces a
 144 “path-and-lag” notation. For example, for $J = 2$ variables $\mathbf{x}_t = (A_t, B_t)$ over $T = 3$ times we
 145 might specify that changing A_t by Δ causes a lagged change of $\gamma\Delta$ in B_{t+1} , represented in path-
 146 and-lag notation as $A \rightarrow B, 1, \beta$. Each one-headed arrow in path-and-lag notation then defines a
 147 path coefficient γ_k that links two variables as represented by $J \times J$ indicator matrix \mathbf{P}_k , and is
 148 also associated with a lag-matrix $\mathbf{L}_{g[k]}$ where $g[k]$ is the specified lag for path coefficient k . In
 149 our example with $K = 1$ path coefficient with a lag-1 effect $g[1] = 1$, this results in:

$$\mathbf{L}_{g[1]} = \begin{bmatrix} 0 & 0 & 0 \\ 1 & 0 & 0 \\ 0 & 1 & 0 \end{bmatrix}, \quad (3)$$

150 and indicator matrix:

$$\mathbf{P}_1 = \begin{bmatrix} 0 & 0 \\ 1 & 0 \end{bmatrix}, \quad (4)$$

151 The joint path matrix is then assembled by summing the contribution of all K path coefficients:

$$\mathbf{P}_{\text{joint}} = \sum_{k=1}^K \gamma_k (\mathbf{L}_{g[k]} \otimes \mathbf{P}_k) \quad (5)$$

152 where \mathbf{P} is a $K \times J \times J$ array containing all indicator matrices \mathbf{P}_k , and $\mathbf{L}_{g[k]} \otimes \mathbf{P}_k$ is the
 153 Kronecker product that results in a $TJ \times TJ$ matrix to match the size of $\mathbf{P}_{\text{joint}}$. In our example,
 154 this results in a joint-path matrix:

$$\mathbf{P}_{\text{joint}} = \begin{bmatrix} 0 & 0 & 0 & 0 & 0 & 0 \\ 0 & 0 & 0 & 0 & 0 & 0 \\ 0 & 0 & 0 & 0 & 0 & 0 \\ 0 & 0 & 0 & 0 & 0 & 0 \\ \gamma_1 & 0 & 0 & 0 & 0 & 0 \\ 0 & \gamma_1 & 0 & 0 & 0 & 0 \end{bmatrix} \quad (6)$$

155 where parameter γ_1 is now duplicated across times.

156 *Moderated variables*

157 Moderated path analysis (Klein & Moosbrugger, 2000) extends the simultaneous equation to
 158 include quadratic terms, $\mathbf{X} = \mathbf{P}_{\text{joint}} \text{vec}(\mathbf{X}) + \text{vec}(\mathbf{X})^T \mathbf{N}_{\text{joint}} \text{vec}(\mathbf{X})$, where \mathbf{N} is an asymmetric
 159 $TJ \times TJ$ matrix that contains quadratic effects. This then allows quadratic relationships among
 160 variables, e.g., $B = \gamma A + \nu A^2$, where γ is the linear in matrix \mathbf{P} and ν is the quadratic effect of A
 161 on B in \mathbf{N} . We specify a moderated structural equation model that has a similar property but
 162 using methods that can be written as a GMRF, as we next show. In particular, we introduce
 163 “path-lag-slope” notation, where e.g., $A \rightarrow B, 0, C$ allows a variable C to replace a stationary
 164 parameter when representing the slope linking A to B .

165 Specifically, we replace a stationary parameter γ_k with a specified model variable \mathbf{x}_j that can
 166 then vary over time. This can be written as:

$$\mathbf{P}_{\text{joint}} = \sum_{k=1}^K (\mathbf{L}_{g[k]} \mathbf{Z}_k) \otimes \mathbf{P}_k \quad (7)$$

167 where:

$$\mathbf{Z}_k = \begin{cases} \gamma_k \mathbf{I} & \text{if path is stationary with value } \gamma_k \\ \text{diag}(\mathbf{x}_{j[k]}) & \text{if path is nonstationary with value } \mathbf{x}_{j[k]} \end{cases} \quad (8)$$

168 and where $\text{diag}(\mathbf{x}_{j[k]})$ constructs a $T \times T$ diagonal matrix from vector $\mathbf{x}_{j[k]}$ for the variable $j[k]$

169 that replaces path coefficient k , such that $\mathbf{L}_{g[k]} \mathbf{Z}_k$ then applies a lag operator $\mathbf{L}_{g[k]}$ such that

170 $x_{t_1 j[k]}$ is the impact of $x_{t_1 j_1}$ on $x_{t_2 j_2}$ where $t_2 \geq t_1$. We propose two interpretations for this

171 expanded specification for DSEM (see Fig. 1 for examples):

172 1. *Random slopes*: The variable $\mathbf{x}_{j[k]}$ that is used instead of path coefficient k could be
 173 interpreted as a random slope (Gelman & Hill, 2007). For example, we might have a model
 174 with $J = 3$ variables, $\mathbf{x}_t = (A_t, B_t, \beta_t)$, where β_t is effect of A_t on B_t , $B_t = \mu_B + \beta_t A_t + \epsilon_t$,
 175 and written as $A \rightarrow B, 0, \text{beta}$ in arrow-lag-slope notation (see Fig. 1B).

176 2. *Product of two variables in a graphical model*: The joint path matrix $\mathbf{P}_{\text{joint}}$ defines a
 177 graphical model, where many edges (arrows representing causal effects) can collide in a
 178 single node (vertex representing a response variable), and this collision corresponds to
 179 adding together the contribution of these multiple predictor-variables to predict a single
 180 response-variable. However, using “moderator” variable $\mathbf{x}_{j[k]}$ to represent the impact of
 181 predictor \mathbf{x}_{k_1} on response \mathbf{x}_{k_2} defines a new operator in the graph, where we instead take the
 182 product of two variables \mathbf{x}_{k_1} and $\mathbf{x}_{j[k]}$ when estimating their impact on \mathbf{x}_{k_2} . This interaction
 183 can be viewed as a “composite variable”, which we visualize as a diamond to distinguish it
 184 from measured (“manifest”) variables as squares or unobserved (“latent”) variables as circles
 185 (see Fig. 1C). For example, we might specify $C_t = \beta_A A_t + \beta_{AB} A_t B_t + \epsilon_t$ by specifying four

186 variables $\mathbf{x}_t = (A_t, B_t, AB_t, C_t)$, and using arrow-lag-slope notation to specify $A \rightarrow AB, 0, B$.

187 The resulting model can be viewed as a time-series version of a multi-level probabilistic

188 graphical model (Koller & Friedman, 2009).

189 These different interpretations arise even when one or more variables has missing values.

190 For example, we might want to estimate the impact of temperature T on other variables.

191 However, species densities might initially increase and then eventually decrease with increases in

192 temperature (a “dome-shaped temperature response”). This can be approximated as a quadratic

193 effect $Y = \beta_T T + \beta_{T^2} T^2$, and we can construct the temperature-squared term as the product of

194 temperature and itself ($T \rightarrow T, 0, T$ in path-lag-slope notation). T^2 is then a latent variable,

195 which is calculated from estimated (imputed) values of T . Alternatively, we can use a third-order

196 Taylor-series (Maclaurin) approximation:

$$e^A \approx \sum_{i=0}^3 \frac{A^i}{i!} \quad (9)$$

197 and using a power-series for covariate A to approximate an exponential function (Fig. 1D), with

198 error bounded by $e^{|A|} \frac{A^4}{4!}$.

199 Defining the path matrix $\mathbf{P}_{\text{joint}}$ using a moderated dynamic structural equation model

200 (MDSEM) allows us to approximate interactions, exponential, and polynomial effects while also

201 interpolating missing data, estimating direct and indirect effects, and constraining model

202 covariance using domain knowledge. The MDSEM is available in the R package *dsem* (Thorson

203 et al., 2024) version 2.0.0, which uses package *TMB* (Kristensen et al., 2016) to calculate the

204 Laplace approximation (Skaug & Fournier, 2006) when calculating the marginal likelihood of

205 parameters while integrating across random effects, and the *Eigen* package to efficiently

206 calculate sparse-matrix computations (Guennebaud et al., 2010). We then optimize the marginal

207 likelihood in the R statistical environment (R Core Team, 2023), and use a generalization of the
208 delta method (Kass & Steffey, 1989) to calculate standard errors for parameters and derived
209 quantities.

210 *Simulation experiment: Autocorrelated random-slopes model*

211 We first confirm that MDSEM can accurately recover a model variable $\mathbf{x}_{j[k]}$ that is treated as a
212 varying slope representing the impact of one variable on another. To do so, we simulation data a
213 “random slopes” time-series model:

$$A_t \sim \text{Normal}(0, \sigma_A^2) \quad (10)$$

$$B_t \sim \text{Normal}(\beta_t A_t, \sigma_B^2)$$

$$\beta_t = 0.5 \left(\sin \left(2\pi \frac{t-1}{T-1} \right) + 1 \right)$$

214 where $\mathbf{x}_t = (A_t, B_t, \beta_t)$ is the set of $J = 3$ variables over $T = 51$ times, and slope β_t fluctuates
215 from $\beta_1 = 1$ to $\beta_{25} = 0$ and back to $\beta_{51} = 1$. We then fit MDSEM observing $\mathbf{y}_t = (A_t, B_t, \text{NA})$ and
216 specifying a first-order autoregressive process on the slope variable. We contrast this with a
217 conventional DSEM fitting the $J = 2$ observed variables and assuming that slope β is stationary
218 over time. We specify $\sigma_A = 1$ and explore three scenarios that have different magnitudes of error
219 in the response, $\sigma_B = \{0.2, 0.5, 1.0\}$. For each scenario, we simulate 500 simulation replicates,
220 and record the estimated $\hat{\beta}_t$ (for the MDSEM) or $\hat{\beta}$ for the (DSEM), and compare these with the
221 known true value.

222 *Case 1: Random slopes linking regional and local habitat*

223 We next demonstrate using MDSEM as a varying slope model using real-world data. To do so,
224 we analyze the relationship between sea surface temperatures at Departure Bay (Vancouver
225 Island, British Columbia, Canada) and a regional climate index (the Pacific Decadal Oscillation,

226 PDO), using annual measurements in January from 1914-2017 (see Table S1 for code). We seek
 227 to estimate how the relationship has changed during 100 years of climate change:

$$X_t \sim \begin{cases} \text{Normal}(\mu_X, \sigma_X^2) & \text{if } t = 1914 \\ \text{Normal}(\rho_X(X_{t-1} - \mu_X) + \mu_X, \sigma_X^2) & \text{if } t > 1914 \end{cases} \quad (11)$$

$$\beta_t \sim \begin{cases} \text{Normal}(\mu_\beta, \sigma_\beta^2) & \text{if } t = 1914 \\ \text{Normal}(\rho_\beta(\beta_{t-1} - \mu_\beta) + \mu_\beta, \sigma_\beta^2) & \text{if } t > 1914 \end{cases}$$

$$Y_t \sim \begin{cases} \text{Normal}(\mu_Y, \sigma_Y^2) & \text{if } t = 1914 \\ \text{Normal}(\rho_Y(Y_{t-1} - \mu_Y) + \beta_t(X_t - \mu_X) + \mu_Y, \sigma_Y^2) & \text{if } t > 1914 \end{cases}$$

228 where we estimate the conditional variance and first-order autocorrelation for each of $J = 3$
 229 variables, where PDO X_t and local temperature Y_t are both observed and β_t is a latent variable
 230 representing the time-varying slope.

231 *Case 2: Lotka-Volterra predator-prey dynamics*

232 We next demonstrate using MDSEM to approximate a mechanistic model that involves a
 233 nonlinear relationship among variables. To do so, we demonstrate it using the Lotka-Volterra
 234 model, which remains one of the most widely-taught descriptions for predator-prey dynamics. It
 235 defines an ordinary differential equation for the abundance of prey X_t and predators Y_t :

$$\frac{d}{dt}X_t = \alpha X_t - \beta X_t Y_t \quad (12)$$

$$\frac{d}{dt}Y_t = \gamma X_t Y_t - \delta Y_t$$

236 where α is the per-capita growth rate for prey, β is the prey mortality per predator-prey
 237 encounter, γ is the predator growth rate per encounter, and δ is the predator mortality rate in the
 238 absence of encounters. We first reformulate in terms of log-abundance:

$$\frac{d}{dt} \log_e(X_t) = \frac{1}{X_t} \frac{d}{dt} X_t = \alpha - \beta Y_t \quad (13)$$

$$\frac{d}{dt} \log_e(Y_t) = \frac{1}{Y_t} \frac{d}{dt} Y_t = \gamma X_t - \delta$$

239 and then use the 3rd-order Taylor series approximation to the exponential function, $\tilde{X}_t =$
 240 $\sum_{i=0}^3 \frac{\log(X_t)^i}{i!}$ and $\tilde{Y}_t = \sum_{i=0}^3 \frac{\log(Y_t)^i}{i!}$. Finally, we use a first-order forwards-Euler approximation to
 241 the ODE, and add process errors representing unmeasured variation in productivity for the prey
 242 ($\epsilon_{t,1}$) or predator ($\epsilon_{t,2}$):

$$\log(X_{t+1}) = \log(X_t) + \alpha - \beta \tilde{Y}_t + \epsilon_{t,1} \quad (14)$$

$$\log(Y_{t+1}) = \log(Y_t) + \gamma \tilde{X}_t - \delta + \epsilon_{t,2}$$

243 where this approximation can be fitted using MDSEM. We then compare MDSEM estimates
 244 $\hat{\theta}_{\text{DSEM}} = (\hat{\alpha}_{\text{DSEM}}, \hat{\beta}_{\text{DSEM}}, \hat{\delta}_{\text{DSEM}}, \hat{\gamma}_{\text{DSEM}})$ with the maximum-likelihood estimate $\hat{\theta}_{\text{ODE}}$ resulting
 245 from a 3rd-order Runge-Kutta ODE solver implemented using RTMB (Kristensen, 2024).

246 We specifically compare $\hat{\theta}_{\text{DSEM}}$ and $\hat{\theta}_{\text{ODE}}$ using two examples:

247 1. *Hare-Lynx in pelt records from Hudson Bay*: We use records of pelts for Canada Lynx and
 248 their prey snowshoe hare from Hudson Bay 1900-1920, extracted from Gotelli (2008 Fig.
 249 6.16) and originating elsewhere (Elton & Nicholson, 1942; MacLulich, 1937);
 250 2. *Didinium-Paramesium microcosm experiment*: We use records of *Paramesium aurelia* and
 251 *Didinium nasutum* in a microcosm experiment at 0.5 Cerophyll concentration measured
 252 every 12 hours over 35 days, i.e., $T = 71$ (Veilleux, 1979 Fig. 11a), as previously digitized
 253 (Jost & Ellner, 2000 Fig. 1).

254 In each case, we randomly drop 10% of measurements to demonstrate the ability to impute
 255 missing values jointly with estimating parameters.

256 *Case 3: Temperature-dependent resource-consumer-predator dynamics*

257 Finally, we demonstrate using MDSEM to estimate how covariates can moderate variation in
 258 slopes over time including polynomial effects. To do so, we estimate a quadratic impact of
 259 temperature on species interactions, using monthly measurements of Temperature (W_t in
 260 Celcius), *Cryptomonas* (resource, C_t in log-abundance), *Daphnia* (consumer, D_t in log-
 261 abundance), and *Leptodora* (predator, L_t in log-abundance) in Lake Washington from 1962-
 262 1994, $T = 396$ (Hampton et al., 2006). We specifically focus on dynamics for *Daphnia*, and
 263 estimate a quadratic impact of temperature on *Cryptomonas* and *Daphnia* abundance:

$$W_t = \rho_W W_{t-1} + \epsilon_{W,t} \quad (15)$$

$$C_t = \mu_C + \rho_C (C_{t-1} - \mu_C) + \alpha_C W_t + \beta_C W_t^2 + \epsilon_{C,t}$$

$$D_t = \mu_D + \rho_D (D_{t-1} - \mu_D) + \alpha_D W_t + \beta_D W_t^2 + \gamma_t (C_t - \mu_C) + \delta_t (L_{t-1} - \mu_L) + \epsilon_{D,t}$$

$$L_t = \mu_L + \rho_L (L_{t-1} - \mu_L) + \epsilon_{L,t}$$

264 We also estimate a simultaneous impact of *Cryptomonas* on *Daphnia* that varies over time
 265 following a quadratic temperature response:

$$\gamma_t = \mu_\gamma + \rho_\gamma (\gamma_{t-1} - \mu_\gamma) + \alpha_\gamma W_t + \beta_\gamma W_t^2 + \epsilon_{\gamma,t} \quad (16)$$

266 and a one-month lagged impact of *Leptodora* on *Daphnia* that also varies over time following a
 267 quadratic temperatures response:

$$\delta_t = \mu_\delta + \rho_\delta (\delta_{t-1} - \mu_\delta) + \alpha_\delta W_t + \beta_\delta W_t^2 + \epsilon_{\delta,t} \quad (16)$$

268 We then use a two-sided Wald test to identify which of the eight temperature parameters are
 269 statistically significant ($p < 0.05$).

270 Results

271 *Simulation experiment: Autocorrelated random-slopes model*

272 The simulation experiment confirms that MDSEM can accurately estimate autocorrelated
 273 variation for a slope parameter measuring the impact of one variable on another (Fig. 2).

274 However, as error in the response variable increases (from left to right panel of Fig. 2): (1) the
275 random-slope estimate shrinks towards the average slope value across time (i.e., red line shrinks
276 towards blue line), and (2) the simulation interval (shaded area) increases in width. Therefore,
277 the ability of MDSEM to estimate a path coefficient as a latent variable depends upon the quality
278 of available data.

279 *Case 1: Random slopes linking regional and local habitat*

280 We first confirm that a time-varying slope can be estimated using a latent variable (e.g.,
281 following an autoregressive process) as the slope parameter. In the random-slopes model
282 predicting sea surface temperature at Departure Bay from the Pacific Decadal Oscillation (Fig.
283 2), the model estimates stronger autocorrelation for the varying slope (0.87) than PDO (0.49) or
284 the conditional errors in temperature (0.11). Inspecting the estimated slope, we see the weakest
285 association from 1915-1925, and a relatively stable slope from 1940-2017 (Fig. 3 3rd row). As
286 expected, estimating a stationary slope (0.37) is nearly the midpoint of the estimated values when
287 allowing the slope to be nonstationary.

288 *Case 2: Lotka-Volterra predator-prey dynamics*

289 We next confirm that we can use latent-moderated interactions to approximate a nonlinear (e.g.,
290 exponential) function with the widely used Lotka-Volterra model for predator-prey dynamics.
291 Comparing interaction estimates from the MDSEM with a state-space solution to the ODE (Fig.
292 4), we see that the two largely agree in sign and magnitude. Differences become more
293 pronounced for larger (> 0.5) estimated interactions, but the estimated carrying capacity is close
294 (and within confidence intervals) for both implementations. Similarly, both models interpolate
295 missing values similarly (Fig. 5), and in a manner that is consistent with the oscillatory dynamics
296 of the system.

297 *Case 3: Temperature-dependent resource-consumer-predator dynamics*

298 Finally, we confirm that we can use latent-moderated interactions to include polynomial
299 covariate effects, specifically specifying a quadratic temperature response on both intercepts
300 (average density) and slopes (interactions) in a resource-consumer-predator model. Inspecting
301 the resulting graph (Fig. 6), we see that linear and quadratic temperature effects are significant
302 for the consumer (*Daphnia*) density, as well as the impact of the resource (*Cryptomonas*) on the
303 consumer, whereas the other temperature responses are not statistically significant. Examining
304 the estimated temperature-response curve (Fig. 7), the two significant effects both have a positive
305 and dome-shaped response, where densities and interactions are highest at 12-14 degrees Celcius
306 (Fig. 7B and 7C). By contrast, the other two temperature-response curves (Fig. 7A and 7C) have
307 a confidence interval that could include a constant value over a large portion of the range of
308 temperatures.

309 **Discussion**

310 In this paper, we demonstrated how a moderated dynamic structural equation model
311 (MDSEM) can extend causal analysis to include nonstationarity, nonlinearity, and statistical
312 interactions, while also interpolating missing values, specifying latent variables, and estimating
313 both simultaneous and lagged relationships among variables. We used a simulation experiment
314 to confirm that sinusoidal variation in a slope linking two variables can be estimated as a
315 autoregressive latent variable, and that the estimated slope is shrunk towards a constant value as
316 data become less informative. We then demonstrated nonstationarity using a time-varying
317 relationship between local and regional climate, nonlinearity using Lotka-Volterra dynamics, and
318 statistical interactions by estimating temperature-dependent interactions in a resource-consumer-
319 predator system. The method is available in an R-package *dsem* (starting with release 2.0.0), and

320 we next discuss how this MDSEM might be useful for a range of theoretical and applied
321 questions throughout ecology.

322 SEM (and its spatial, phylogenetic, and time-series extensions) are useful for applied
323 ecologists because they address several drawbacks of conventional linear regression (e.g.,
324 generalized linear models and analysis of variance). In particular, SEM addresses the problem of
325 collinearity (Dormann et al., 2013) by using domain knowledge to inform predictions given
326 novel combinations of predictors, and also accounts for missing values for both predictor and
327 response variables by specifying a joint distribution for both. Despite these advantages,
328 phylogenetic, spatial, and time-series applications of SEM have previously lacked any capability
329 to estimate nonlinearity, nonstationarity, and statistical interactions, which are also of general
330 interest in ecology. By addressing these challenges, moderated SEM seems suitable for the wide
331 range of uses discussed in recent ecological reviews (Arif & MacNeil, 2022; Byrnes & Dee,
332 2025; Grace, 2024; Larsen et al., 2019). In particular, DSEM has previously required assuming
333 that path coefficients (i.e., simultaneous and lagged interactions among variables) are constant
334 over time. After developing a DSEM based on scientific knowledge, we recommend that
335 analysts sequentially test the model when replacing each path coefficient with a model variable
336 (e.g., which follows an autoregressive process), and use model selection to evaluate the strength
337 of evidence that the path coefficient is stationary or varies over time.

338 In addition to a growing interest in causal analysis using SEM and PA, ecologists use
339 custom-built hierarchical models (i.e., integrated-population or stock-assessment models [IPMs])
340 to predict the likely effect of hypothetical policy changes (Kéry & Schaub, 2021). IPMs are a
341 powerful tool for applied ecologists because they allow analysts to incorporate nonlinear and
342 state-space features that are specifically suited to their study system. However, IPMs are often

343 specified using Bayesian hierarchical modelling, which then requires specifying a directed
344 acyclic graph (DAG) for linkages among system components (i.e., avoiding cyclic dependencies
345 among system variables). By contrast, SEM (including DSEM and MDSEM) can estimate these
346 cyclic dependencies ($A \rightarrow B \rightarrow C \rightarrow A$) while simultaneously imputing missing variables.
347 Additionally, the “arrow-lag-slope” notation developed here continues to provide a high-level
348 interface for specifying system linkages using MDSEM. We believe that a simple and expressive
349 interface is necessary for broad adoption of any statistical tool for ecologists, similar to how the
350 ‘formula’ interface for linear models (Wilkinson & Rogers, 1973) has led to broad adoption
351 among ecologists of linear mixed and generalized additive models. Ultimately, we envision
352 embedding MDSEM as an interface to specify linkages among process errors and/or covariates
353 for use within IPMs (Champagnat et al., 2025).

354 Finally, we showed how the output of MDSEM can be plotted to summarize context-
355 dependent and nonstationary relationships (e.g., Fig 2, 6, and S1). However, analysts will also
356 want to compute the total effect of an exogenous (policy) change in system variables. In
357 conventional DSEM, the total effect is computed from the $\mathbf{P}_{\text{joint}}$, which is assumed to be
358 stationary over time. Specifically, an analyst might envision a policy that changes the states \mathbf{X} to
359 $\mathbf{X} + \mathbf{D}$, where change-matrix \mathbf{D} could represent a pulse experiment (i.e., non-zero values in only
360 a single time) or press experiment (i.e., non-zero values continuing indefinitely). This change
361 causes in a first-order effect $\mathbf{P}_{\text{joint}} \text{vec}(\mathbf{D})$, which in turn causes a second-order effect
362 $\mathbf{P}_{\text{joint}}^2 \text{vec}(\mathbf{D})^T$, and where the total effects is then $(\mathbf{I} - \mathbf{P}_{\text{joint}})^{-1} \text{vec}(\mathbf{D})$. By contrast, MDSEM
363 allows $\mathbf{P}_{\text{joint}}$ to vary due to other latent or endogenous variables. Computing the total effect
364 therefore involves a first-order effect, $\mathbf{P}_1 \text{vec}(\mathbf{D})$ where $\mathbf{P}_1 = \mathbf{P}_{\text{joint}}$. However, the second-order
365 effect requires updated path matrix \mathbf{P}_2 , calculated by updating $\mathbf{P}_{\text{joint}}$ given the previous first-

366 order effects (Eq. 5A-5B), where the second-order effect is $\mathbf{P}_2 \mathbf{P}_1 \text{vec}(\mathbf{D})$. By extension, the total
367 effect is the sum across all such partial effects, $\text{vec}(\mathbf{D})^T (\sum_{k=1}^{\infty} \prod_{k'=1}^k \mathbf{P}_{k'})$. We therefore
368 acknowledge that interpreting the total effect is more complicated in moderated SEM than in
369 conventional cases.

370 **References**

371 Arif, S., & MacNeil, M. A. (2022). Predictive models aren't for causal inference. *Ecology Letters*, 25(8), 1741–1745. <https://doi.org/10.1111/ele.14033>

372 Arif, S., & MacNeil, M. A. (2023). Applying the structural causal model framework for
373 observational causal inference in ecology. *Ecological Monographs*, 93(1), e1554.
374 <https://doi.org/10.1002/ecm.1554>

375 Asparouhov, T., Hamaker, E. L., & Muthén, B. (2018). Dynamic Structural Equation Models.
376 *Structural Equation Modeling: A Multidisciplinary Journal*, 25(3), 359–388.
377 <https://doi.org/10.1080/10705511.2017.1406803>

378 Byrnes, J. E. K., & Dee, L. E. (2025). Causal Inference With Observational Data and
379 Unobserved Confounding Variables. *Ecology Letters*, 28(1), e70023.
380 <https://doi.org/10.1111/ele.70023>

381 Champagnat, J., Monnahan, C. C., Sullivan, J. Y., Thorson, J. T., Shotwell, K. S., Rogers, L. A.,
382 & Punt, A. E. (2025). *Causal models as a scientific framework for next-generation*
383 *ecosystem and climate-linked stock assessments*.
384 <https://ecoenvorxiv.org/repository/view/9794/>

385 Dormann, C. F., Elith, J., Bacher, S., Buchmann, C., Carl, G., Carré, G., Marquéz, J. R. G.,
386 Gruber, B., Lafourcade, B., Leitão, P. J., Münkemüller, T., McClean, C., Osborne, P. E.,
387 Reineking, B., Schröder, B., Skidmore, A. K., Zurell, D., & Lautenbach, S. (2013).

389 Collinearity: A review of methods to deal with it and a simulation study evaluating their
390 performance. *Ecography*, 36(1), 27–46. <https://doi.org/10.1111/j.1600-0587.2012.07348.x>

391

392 Elton, C., & Nicholson, M. (1942). The Ten-Year Cycle in Numbers of the Lynx in Canada.
393 *Journal of Animal Ecology*, 11(2), 215–244. <https://doi.org/10.2307/1358>

394 Gelman, A., & Hill, J. (2007). *Data analysis using regression and multilevel/hierarchical*
395 *models*. Cambridge University Press.

396 Gotelli, N. J. (2008). *A Primer of Ecology, Fourth Edition by Nicholas J. Gotelli*. Sinauer
397 Associates, 2008.

398 Grace, J. B. (2024). An integrative paradigm for building causal knowledge. *Ecological*
399 *Monographs*, 94(4), e1628. <https://doi.org/10.1002/ecm.1628>

400 Guennebaud, G., Jacob, B., & others. (2010). *Eigen v3*. <http://eigen.tuxfamily.org>

401 Hampton, S. E., Scheuerell, M. D., & Schindler, D. E. (2006). Coalescence in the Lake
402 Washington story: Interaction strengths in a planktonic food web. *Limnology and*
403 *Oceanography*, 51(5), 2042–2051. <https://doi.org/10.4319/lo.2006.51.5.2042>

404 Hixon, M. A., & Carr, M. H. (1997). Synergistic predation, density dependence, and population
405 regulation in marine fish. *Science*, 277(5328), 946.

406 Holmes, E. E., Ward, E. J., & Wills, K. (2012). Marss: Multivariate autoregressive state-space
407 models for analyzing time-series data. *The R Journal*, 4, 11–19.

408 Ives, A. R. (2022). Random errors are neither: On the interpretation of correlated data. *Methods*
409 *in Ecology and Evolution*, 13(10), 2092–2105. <https://doi.org/10.1111/2041-210X.13971>

410 Ives, A. R., Dennis, B., Cottingham, K. L., & Carpenter, S. R. (2003). Estimating community
411 stability and ecological interactions from time-series data. *Ecological Monographs*,
412 73(2), 301–330.

413 Jost, C., & Ellner, S. P. (2000). Testing for predator dependence in predator-prey dynamics: A
414 non-parametric approach. *Proceedings of the Royal Society of London. Series B:*
415 *Biological Sciences*. <https://doi.org/10.1098/rspb.2000.1186>

416 Kass, R. E., & Steffey, D. (1989). Approximate Bayesian inference in conditionally independent
417 hierarchical models (parametric empirical bayes models). *Journal of the American
418 Statistical Association*, 84(407), 717–726. <https://doi.org/10.2307/2289653>

419 Kéry, M., & Schaub, M. (2021). *Integrated population models: Theory and ecological
420 applications with R and JAGS* (1st edition). Academic Press.

421 Klein, A., & Moosbrugger, H. (2000). Maximum Likelihood Estimation of Latent Interaction
422 Effects with the LMS Method. *Psychometrika*, 65(4), 457–474.
423 <https://doi.org/10.1007/BF02296338>

424 Koller, D., & Friedman, N. (2009). *Probabilistic graphical models: Principles and techniques*.
425 MIT press.
426 https://books.google.com/books?hl=en&lr=&id=7dzpHCHzNQ4C&oi=fnd&pg=PR9&dq=Probabilistic+Graphical+Models+Principles+and+Techniques&ots=py4Cxn2-zM&sig=gptWuvP1MZ_ebACxp7A71XG0tzM

429 Kristensen, K. (2024). *RTMB: “R” Bindings for “TMB.”* [https://CRAN.R-
430 project.org/package=RTMB](https://CRAN.R-project.org/package=RTMB)

431 Kristensen, K., Nielsen, A., Berg, C. W., Skaug, H., & Bell, B. M. (2016). TMB: Automatic
432 differentiation and Laplace approximation. *Journal of Statistical Software*, 70(5), 1–21.
433 <https://doi.org/10.18637/jss.v070.i05>

434 Larsen, A. E., Meng, K., & Kendall, B. E. (2019). Causal analysis in control–impact ecological
435 studies with observational data. *Methods in Ecology and Evolution*, 10(7), 924–934.
436 <https://doi.org/10.1111/2041-210X.13190>

437 Lefcheck, J. S. (2016). piecewiseSEM: Piecewise structural equation modelling in r for ecology,
438 evolution, and systematics. *Methods in Ecology and Evolution*, 7(5), 573–579.
439 <https://doi.org/10.1111/2041-210X.12512>

440 MacLulich, D. A. (1937). *Fluctuations in the Numbers of the Varying Hare (Lepus Americanus)*.
441 University of Toronto Press. <https://doi.org/10.3138/9781487583064>

442 Mahaffy, J. (2009). *Qualitative Analysis of the Lotka–Volterra Equations*. San Diego State
443 University. <https://jmahaffy.sdsu.edu/courses/f09/math636/lectures/lotka/qualde2.html>

444 Munch, S. B., Giron-Nava, A., & Sugihara, G. (2018). Nonlinear dynamics and noise in fisheries
445 recruitment: A global meta-analysis. *Fish and Fisheries*, 19(6), 964–973.
446 <https://doi.org/10.1111/faf.12304>

447 Papadogeorgou, G., Bello, C., Ovaskainen, O., & Dunson, D. B. (2023). Covariate-Informed
448 Latent Interaction Models: Addressing Geographic & Taxonomic Bias in Predicting
449 Bird–Plant Interactions. *Journal of the American Statistical Association*, 118(544), 2250–
450 2261. <https://doi.org/10.1080/01621459.2023.2208390>

451 R Core Team. (2023). *R: A Language and Environment for Statistical Computing*. R Foundation
452 for Statistical Computing. <https://www.R-project.org/>

453 Rollinson, C. R., Finley, A. O., Alexander, M. R., Banerjee, S., Dixon Hamil, K.-A., Koenig, L.
454 E., Locke, D. H., DeMarche, M. L., Tingley, M. W., Wheeler, K., Youngflesh, C., &
455 Zipkin, E. F. (2021). Working across space and time: Nonstationarity in ecological
456 research and application. *Frontiers in Ecology and the Environment*, 19(1), 66–72.
457 <https://doi.org/10.1002/fee.2298>

458 Skaug, H., & Fournier, D. (2006). Automatic approximation of the marginal likelihood in non-
459 Gaussian hierarchical models. *Computational Statistics & Data Analysis*, 51(2), 699–709.

460 Thorson, J. T., Anderson, S. C., Goddard, P., & Rooper, C. N. (2025). tinyVAST: R Package With
461 an Expressive Interface to Specify Lagged and Simultaneous Effects in Multivariate
462 Spatio-Temporal Models. *Global Ecology and Biogeography*, 34(4), e70035.
463 <https://doi.org/10.1111/geb.70035>

464 Thorson, J. T., Andrews III, A. G., Essington, T. E., & Large, S. I. (2024). Dynamic structural
465 equation models synthesize ecosystem dynamics constrained by ecological mechanisms.
466 *Methods in Ecology and Evolution*, 15(4), 744–755. <https://doi.org/10.1111/2041-210X.14289>

468 Thorson, J. T., Ciannelli, L., & Litzow, M. A. (2020). Defining indices of ecosystem variability
469 using biological samples of fish communities: A generalization of empirical orthogonal
470 functions. *Progress in Oceanography*, 181, 102244.
471 <https://doi.org/10.1016/j.pocean.2019.102244>

472 Thorson, J. T., Maureaud, A. A., Frelat, R., Mérigot, B., Bigman, J. S., Friedman, S. T.,
473 Palomares, M. L. D., Pinsky, M. L., Price, S. A., & Wainwright, P. (2023). Identifying
474 direct and indirect associations among traits by merging phylogenetic comparative

475 methods and structural equation models. *Methods in Ecology and Evolution*, 14(5), 1259–
476 1275. <https://doi.org/10.1111/2041-210X.14076>

477 Veilleux, B. G. (1979). An Analysis of the Predatory Interaction Between Paramecium and
478 Didinium. *Journal of Animal Ecology*, 48(3), 787–803. <https://doi.org/10.2307/4195>

479 von Hardenberg, A., & Gonzalez-Voyer, A. (2013). Disentangling evolutionary cause-effect
480 relationships with phylogenetic confirmatory path analysis. *Evolution; International
481 Journal of Organic Evolution*, 67(2), 378–387. <https://doi.org/10.1111/j.1558->
482 5646.2012.01790.x

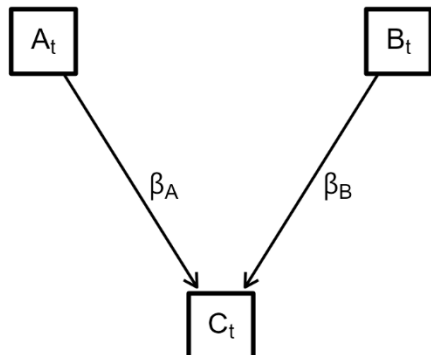
483 Wilkinson, G. N., & Rogers, C. E. (1973). Symbolic Description of Factorial Models for
484 Analysis of Variance. *Journal of the Royal Statistical Society Series C: Applied Statistics*,
485 22(3), 392–399. <https://doi.org/10.2307/2346786>

486 Wootton, J. T., & Emmerson, M. (2005). Measurement of interaction strength in nature. *Annual
487 Review of Ecology, Evolution, and Systematics*, 419–444.

488

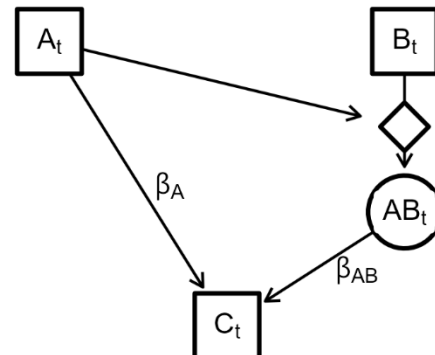
489 Fig. 1 – Graphical models illustrating potential uses for latent-moderated dynamic structural
 490 equation models (MDSEM), where measured (“manifest”) variables are boxes, unmeasured
 491 (“latent”) variables are circles, varying slopes (“latent-moderated paths”) are diamonds,
 492 and arrows point from predictor to response variable while listing either a Greek symbol
 493 (representing an estimated parameter) or a Arabic numeral (representing a value that is fixed a
 494 priori), and also showing the resulting equations below each panel. We contrast the simple case
 495 of a regression model with two independent predictors (panel A), a regression with a statistical
 496 interaction (panel B), a regression with a randomly varying slope (panel C), and a 3rd-order
 497 Taylor series approximation to the exponential function (panel D).

(A) Additive



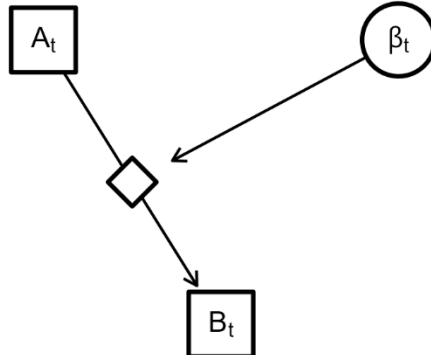
$$C_t = \beta_A A_t + \beta_B B_t + \varepsilon_t$$

(B) Interaction



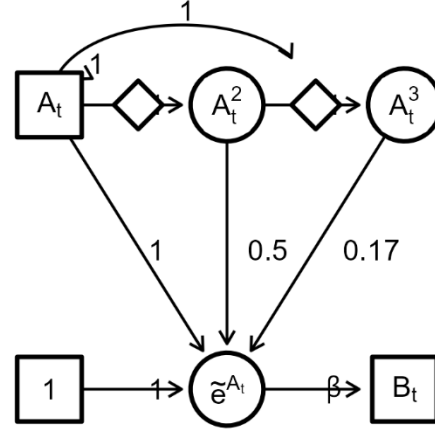
$$C_t = \beta_A A_t + \beta_{AB} A_t B_t + \varepsilon_t$$

(C) Varying slope



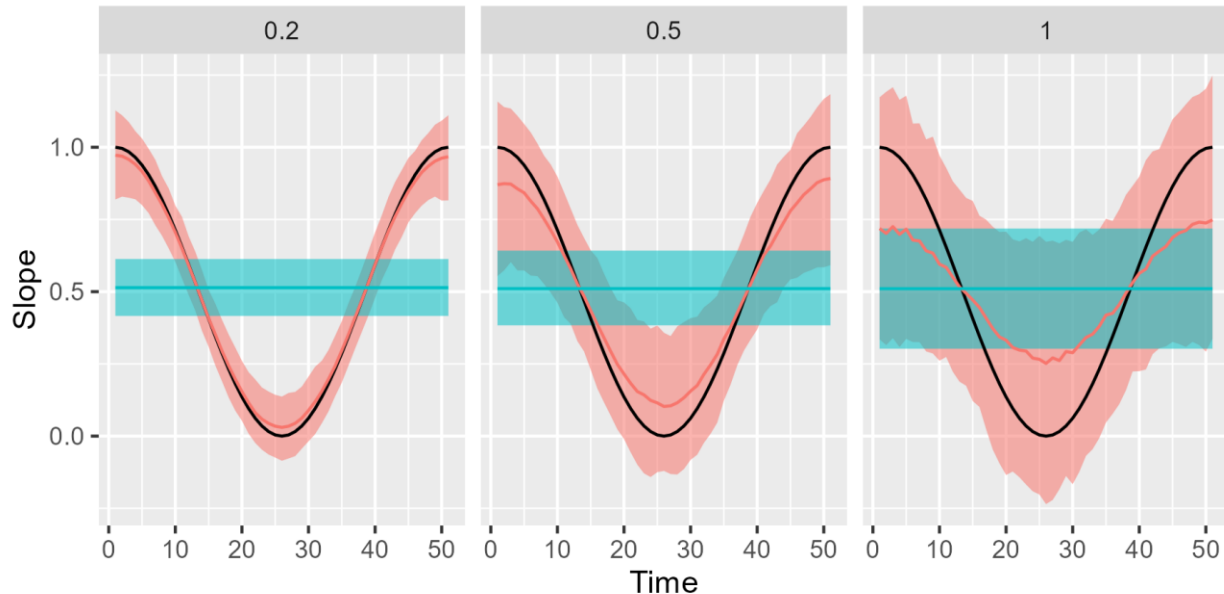
$$C_t = \beta_t A_t + \varepsilon_t$$

(D) Approximated exponential



$$B_t = \beta \tilde{e}^{A_t} + \varepsilon_t$$

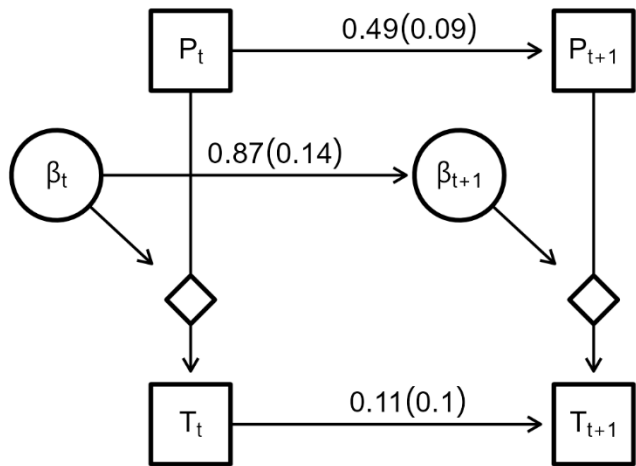
499 Fig. 2 – Results from a simulation experiment involving a random slope model, $A_t = \beta_t B_t + \epsilon_t$
500 where slope β_t (y-axis) follows a sinusoidal pattern (black line) over 50 times (x-axis), and we
501 vary the standard deviation of process errors ϵ_t from low ($\sigma_B = 0.2$, left panel) to medium ($\sigma_B =$
502 0.5, middle panel) or high ($\sigma_B = 1$, right panel) levels, while estimating either a first-order
503 autoregressive process for the slope (red line and shading) or a constant slope (blue line and
504 shading), where the lines show the mean across 500 simulation replicates, and the shading shows
505 the 10% and 90% simulation interval for each model.



506

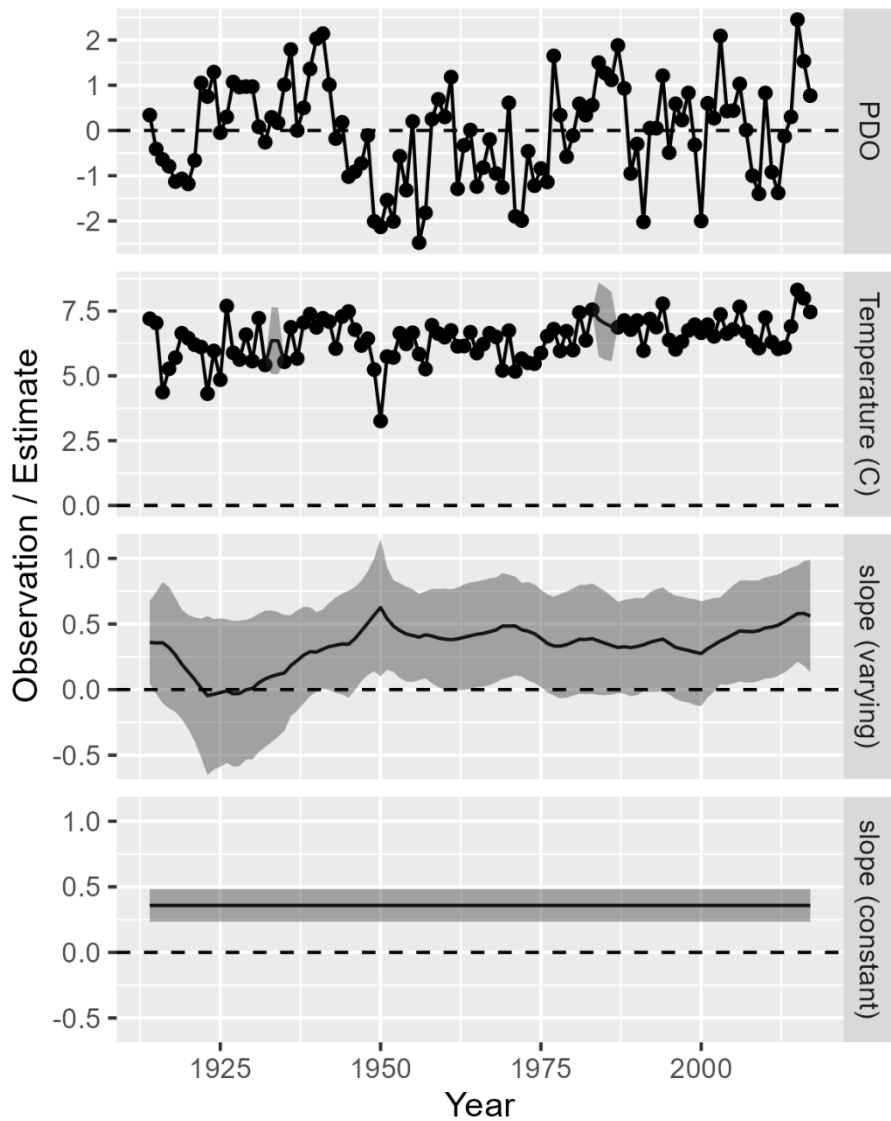
507

508 Fig. 2 – Graphical model and parameter estimates for case study #1, where the Pacific Decadal
509 Oscillation (P_t) is used to predict sea surface temperature at Departure Bay (T_t) with a slope (β_t)
510 that varies as a first-order autoregressive process over time (see Fig. 1 for details about graphical
511 notation).



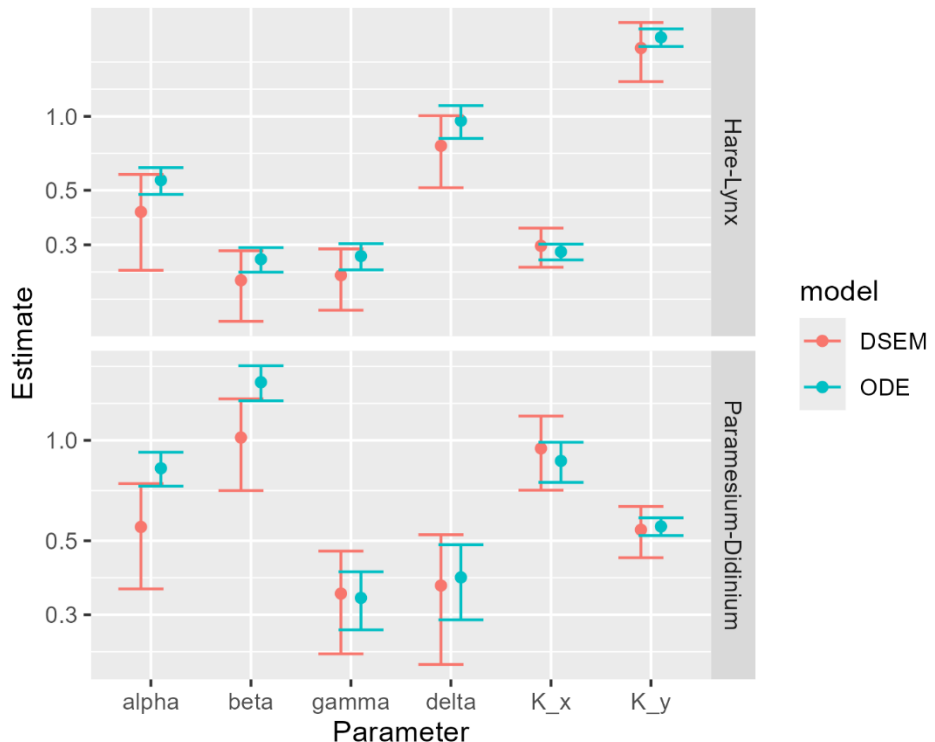
512

513 Fig. 3 – Observed values (circles), estimated values (lines), and 95% confidence intervals
514 (shaded area) for case study #1, showing the Pacific Decadal Oscillation (PDO; top panel),
515 Temperature (2nd panel), and estimated slope (3rd panel), contrasted with the slope estimated by
516 an alternative model when assuming that it is stationary over time (4th panel), and using a shared
517 y-axis scale for the slope estimates (3rd and 4th panels).



518
519
520

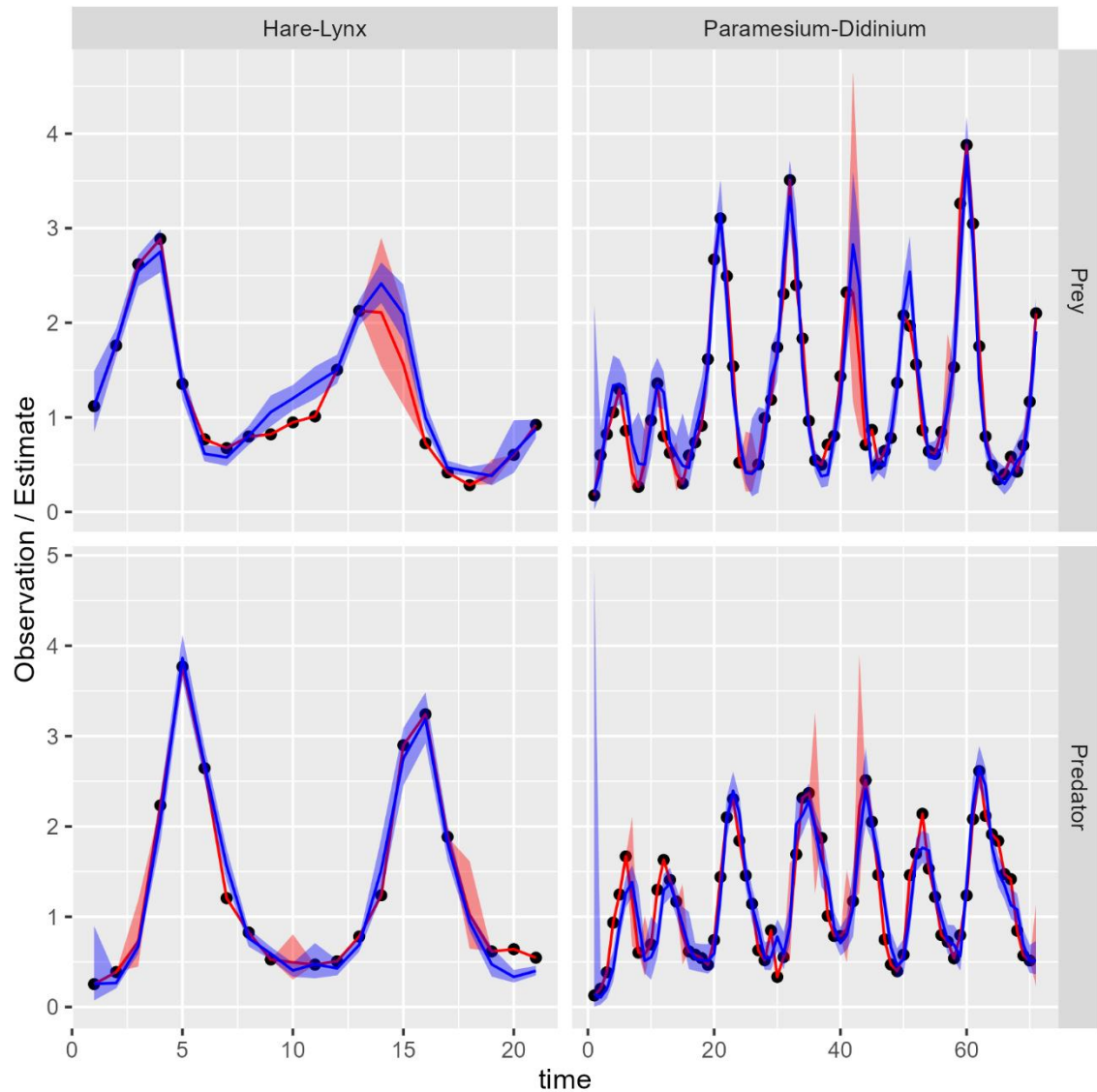
522 Fig. 4 – Estimated interaction parameters ($\alpha, \beta, \gamma, \delta$, dots) and 95% confidence intervals
 523 (whiskers) for case study #2 involving Lotka-Volterra dynamics, as well as the predicted carrying
 524 capacity for the prey $K_x = \frac{\alpha}{\beta}$ and predator $K_y = \frac{\gamma}{\delta}$, estimated using the latent-moderated
 525 dynamic structural equation model with a Taylor-series approximation to a nonlinear
 526 (exponential) function (red) or a state-space ODE model (blue), for each of two case studies
 527 involving Hare-Lynx dynamics in Hudson Bay (top panel), or a Paramesium-Didinium
 528 microcosm experiment (bottom panel)



529

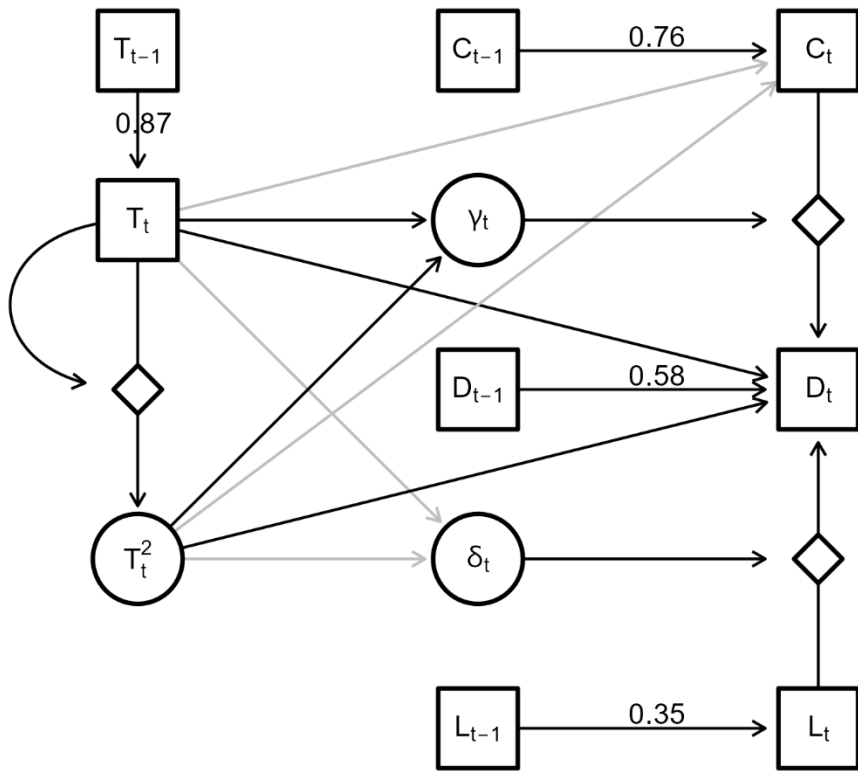
530

531 Fig. 5 -- Observed values (circles), estimated values (lines), and 95% confidence intervals
532 (shaded area) for case study #2 involving Lotka-Volterra dynamics, contrasting estimates using
533 the latent-moderated dynamic structural equation model (red) or the state-space ODE model
534 (blue). Note that the MDSEM assumes that measurements are provided without error and hence
535 only shows confidence intervals for the 10% of observations that were randomly selected and
536 dropped prior to fitting the model.



537

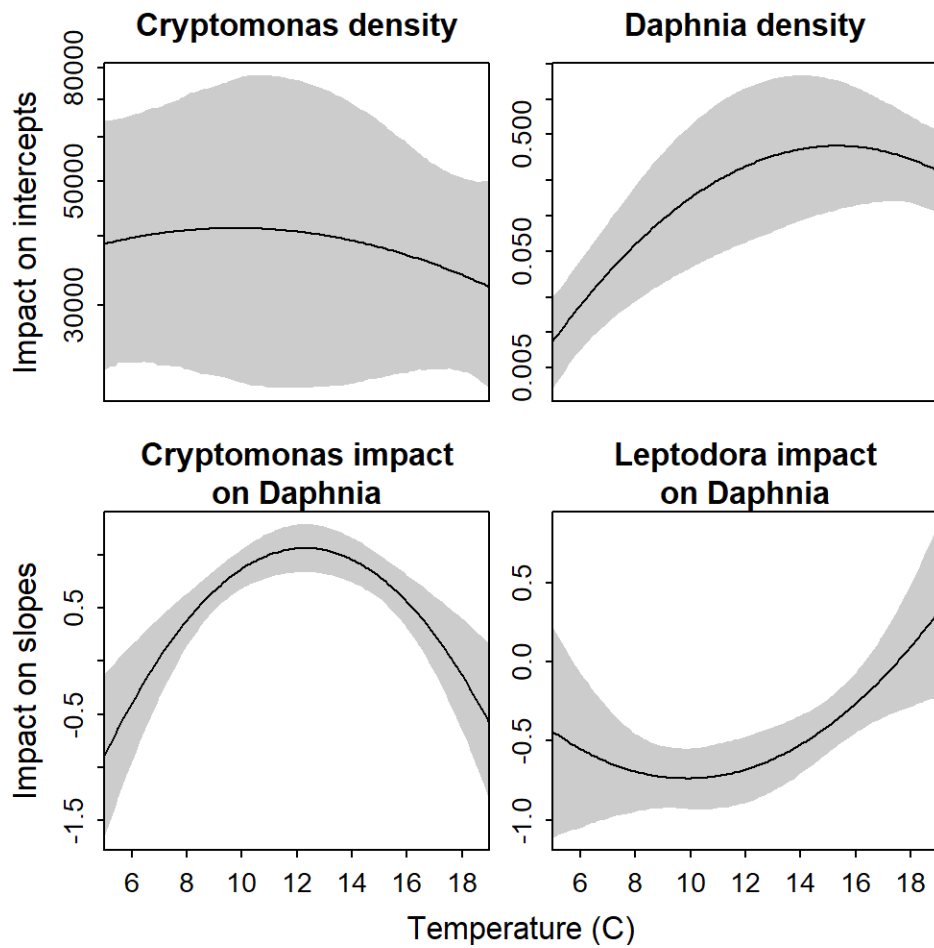
538 Fig. 6 – Graphical model and parameter estimates for case study #3 involving temperature-
 539 dependent resource-consumer-predator interactions (see Fig. 1 for details about graphical
 540 notation), showing Temperature T_t and its polynomial expansion as latent variable T_t^2 , resource
 541 Chryptomonas C_t , consumer $Dapnia D_t$, and predator $Leptodora L_t$, and showing the time-
 542 varying impact of resource on consumers γ_t or predators on consumers δ_t . We also distinguish
 543 linkages (arrows) that are statistically significant (black arrows) or not (grey arrows).



544

545

546 Fig. 7 – Estimated quadratic temperature-response curves (lines) and 95% confidence intervals
547 (shaded area), showing the temperature impact on resource (top-left), consumers (top-right), the
548 impact of resource on consumers (bottom-left), and the impact of predators on consumers
549 (bottom-right)



550

551

552 Table S1: Illustrating the code used to fit case study #1, including the arrow-lag-slope notation
553 (left column), defining a time-series object including all variables (right column top), and the call
554 to package *dsem* to fit the model (right column bottom).

Case 1: Varying slopes

```
# Model  
sem = "  
  PDO -> Temp, 0, slope  
  slope -> slope, 1, ar_slope  
  PDO -> PDO, 1, ar_PDO  
  Temp -> Temp, 1, ar_Temp  
"  
  
# Data  
tsdata = ts(data.frame(  
  Temp = Combo[,2],  
  PDO = Combo[,3],  
  slope = NA  
, start = 1914 ))  
  
# Fit  
fit = dsem(  
  tsdata = tsdata,  
  sem = sem,  
  estimate_mu = c("Temp","PDO","slope")  
)
```

555

556

557 Table S2: Illustrating the code used to fit case study #2 (see Table S1 caption for more details).

Case 2: Lotka-Volterra

```

# Model
sem =
# Main interactions
logX -> logX, 1, NA, 1
ones -> logX, 0, alpha
Y -> logX, 1, beta, -0.1

# Form X \approx exp(logX)
ones -> X, 0, NA, 1
logX -> logX1, 0, NA, 1
logX1 -> X, 0, NA, 1
logX1 -> logX2, 0, logX
logX2 -> X, 0, NA, 0.5
logX2 -> logX3, 0, logX
logX3 -> X, 0, NA, 0.166

# Variances
X <-> X, 0, NA, 0.001
logX <-> logX, 0, sd_logX
logX1 <-> logX1, 0, NA, 0.001
logX2 <-> logX2, 0, NA, 0.001
logX3 <-> logX3, 0, NA, 0.001

# Main interactions
logY -> logY, 1, NA, 1
X -> logY, 1, gamma
ones -> logY, 0, delta, -0.1

# Form Y \approx exp(logY)
ones -> Y, 0, NA, 1
logY -> logY1, 0, NA, 1
logY1 -> Y, 0, NA, 1
logY1 -> logY2, 0, logY
logY2 -> Y, 0, NA, 0.5
logY2 -> logY3, 0, logY
logY3 -> Y, 0, NA, 0.166

# Variances
Y <-> Y, 0, NA, 0.001
logY <-> logY, 0, sd_logY
logY1 <-> logY1, 0, NA, 0.001
logY2 <-> logY2, 0, NA, 0.001
logY3 <-> logY3, 0, NA, 0.001

# Data
Z = cbind(
  logX = log(dat$X),
  logY = log(dat$Y),
  X = NA,
  Y = NA,
  logX1 = NA,
  logY1 = NA,
  logX2 = NA,
  logY2 = NA,
  logX3 = NA,
  logY3 = NA,
  ones = 1
)

# Fit
fit = dsem(
  tsdata = ts(Z),
  sem = sem,
  estimate_mu = vector(),
)

```

```
# Dummy constant
ones <-> ones, 0, NA, 0.001
ones -> ones, 1, NA, 1
"
```

558

559

560

561 Table S3: Illustrating the code used to fit case study #3 (see Table S1 caption for more details).

Case 3: Temperature-dependent resource-consumer-predator

```

# Model
sem = "
# Temperature effect on resource density
Temp -> Cryptomonas, 0, T_to_C
Temp2 -> Cryptomonas, 0, T2_to_C

# Temperature effect on consumer density
Temp -> Daphnia, 0, T_D
Temp2 -> Daphnia, 0, T2_D

# Impacts on consumer
Cryptomonas -> Daphnia, 0, alpha # C_D
Leptodora -> Daphnia, 1, beta # alpha

# Density dependence
Cryptomonas -> Cryptomonas, 1, ar_C
Daphnia -> Daphnia, 1, ar_D
Leptodora -> Leptodora, 1, ar_L

# Form Temp^2
Temp -> Temp2, 0, Temp
Temp2 <-> Temp2, 0, NA, 0.001

# Temperature on resource-consumer slope
alpha <-> alpha, 0, NA, 0.001
Temp -> alpha, 0, T_alpha
Temp2 -> alpha, 0, T2_alpha

# Temperature on predator-consumer slope
beta <-> beta, 0, NA, 0.001
Temp -> beta, 0, T_beta
Temp2 -> beta, 0, T2_beta
"

```

```

# Data
Z = ts(cbind(
  dat$Temp,
  dat$Daphnia,
  dat$Leptodora,
  dat$Cryptomonas,
  alpha = NA,
  Temp2 = NA,
  beta = NA
), start = 1962, freq = 12)

# Fit
fit = dsem(
  tsdata = Z,
  sem = sem,
  estimate_mu = c(
    "Daphnia",
    "Leptodora",
    "Cryptomonas",
    "alpha",
    "beta"
  )
)

```

562

563

564 Table S4: Estimated path coefficients for the Departure Bay case study involving a varying-
 565 slope model linking the Pacific Decadal Oscillation (PDO) to temperatures at a lighthouse near
 566 Departure Bay, listing the model path (first column), time lag (2nd column), parameter name (3rd
 567 column), maximum-likelihood estimate and asymptotic standard error (4th and 5th columns), and
 568 the z-value and p-value from a two-sided Wald test (6th and 7th columns), where columns 4-7 are
 569 NA for parameters that are either fixed, or which vary over time (i.e., the parameter Name
 570 matches a model variable, such as the 1st row).

Path	Lag	Name	Estimate	Std_Error	z_value	p_value
PDO -> Temp	0	slope	NA	NA	NA	NA
slope -> slope	1	ar_slope	0.869	0.142	6.105	0
PDO -> PDO	1	ar_PDO	0.487	0.088	5.529	0
Temp -> Temp	1	ar_Temp	0.112	0.099	1.133	0.257
Temp <-> Temp	0	V[Temp]	0.637	0.055	11.618	0
PDO <-> PDO	0	V[PDO]	0.967	0.067	14.339	0
slope <-> slope	0	V[slope]	0.119	0.082	1.453	0.146

571

572

573 Table S5: Estimated path coefficients for the Lynx-Hare case study involving Lotka-Volterra
 574 predator-prey dynamics (see Table S4 caption for details)

Path	Lag	Name	Estimate	Std_Error	z_value	p_value
logX -> logX	1	NA	1	NA	NA	NA
ones -> logX	0	alpha	0.39	0.079	4.925	0
Y -> logX	1	beta	-0.32	0.05	-6.382	0
ones -> X	0	NA	1	NA	NA	NA
logX -> logX1	0	NA	1	NA	NA	NA
logX1 -> X	0	NA	1	NA	NA	NA
logX1 -> logX2	0	logX	NA	NA	NA	NA
logX2 -> X	0	NA	0.5	NA	NA	NA
logX2 -> logX3	0	logX	NA	NA	NA	NA
logX3 -> X	0	NA	0.166	NA	NA	NA
X <-> X	0	NA	0.001	NA	NA	NA
logX <-> logX	0	sd_logX	0.225	0.037	6.025	0
logX1 <-> logX1	0	NA	0.001	NA	NA	NA
logX2 <-> logX2	0	NA	0.001	NA	NA	NA
logX3 <-> logX3	0	NA	0.001	NA	NA	NA
logY -> logY	1	NA	1	NA	NA	NA
X -> logY	1	gamma	0.639	0.105	6.075	0
ones -> logY	0	delta	-0.765	0.142	-5.372	0
ones -> Y	0	NA	1	NA	NA	NA
logY -> logY1	0	NA	1	NA	NA	NA
logY1 -> Y	0	NA	1	NA	NA	NA
logY1 -> logY2	0	logY	NA	NA	NA	NA
logY2 -> Y	0	NA	0.5	NA	NA	NA
logY2 -> logY3	0	logY	NA	NA	NA	NA
logY3 -> Y	0	NA	0.166	NA	NA	NA
Y <-> Y	0	NA	0.001	NA	NA	NA
logY <-> logY	0	sd_logY	0.352	0.06	5.908	0
logY1 <-> logY1	0	NA	0.001	NA	NA	NA
logY2 <-> logY2	0	NA	0.001	NA	NA	NA
logY3 <-> logY3	0	NA	0.001	NA	NA	NA
ones <-> ones	0	NA	0.001	NA	NA	NA
ones -> ones	1	NA	1	NA	NA	NA

576 Table S6: Estimated path coefficients for the Didinium-Paramecium case study involving Lotka-
 577 Volterra predator-prey dynamics (see Table S4 caption for details)

Path	Lag	Name	Estimate	Std_Error	z_value	p_value
logX -> logX	1	NA	1	NA	NA	NA
ones -> logX	0	alpha	0.523	0.105	5.001	0
Y -> logX	1	beta	-0.44	0.078	-5.611	0
ones -> X	0	NA	1	NA	NA	NA
logX -> logX1	0	NA	1	NA	NA	NA
logX1 -> X	0	NA	1	NA	NA	NA
logX1 -> logX2	0	logX	NA	NA	NA	NA
logX2 -> X	0	NA	0.5	NA	NA	NA
logX2 -> logX3	0	logX	NA	NA	NA	NA
logX3 -> X	0	NA	0.166	NA	NA	NA
X <-> X	0	NA	0.001	NA	NA	NA
logX <-> logX	0	sd_logX	0.429	0.038	11.143	0
logX1 <-> logX1	0	NA	0.001	NA	NA	NA
logX2 <-> logX2	0	NA	0.001	NA	NA	NA
logX3 <-> logX3	0	NA	0.001	NA	NA	NA
logY -> logY	1	NA	1	NA	NA	NA
X -> logY	1	gamma	0.302	0.058	5.238	0
ones -> logY	0	delta	-0.361	0.083	-4.351	0
ones -> Y	0	NA	1	NA	NA	NA
logY -> logY1	0	NA	1	NA	NA	NA
logY1 -> Y	0	NA	1	NA	NA	NA
logY1 -> logY2	0	logY	NA	NA	NA	NA
logY2 -> Y	0	NA	0.5	NA	NA	NA
logY2 -> logY3	0	logY	NA	NA	NA	NA
logY3 -> Y	0	NA	0.166	NA	NA	NA
Y <-> Y	0	NA	0.001	NA	NA	NA
logY <-> logY	0	sd_logY	0.406	0.036	11.15	0
logY1 <-> logY1	0	NA	0.001	NA	NA	NA
logY2 <-> logY2	0	NA	0.001	NA	NA	NA
logY3 <-> logY3	0	NA	0.001	NA	NA	NA
ones <-> ones	0	NA	0.001	NA	NA	NA
ones -> ones	1	NA	1	NA	NA	NA

578

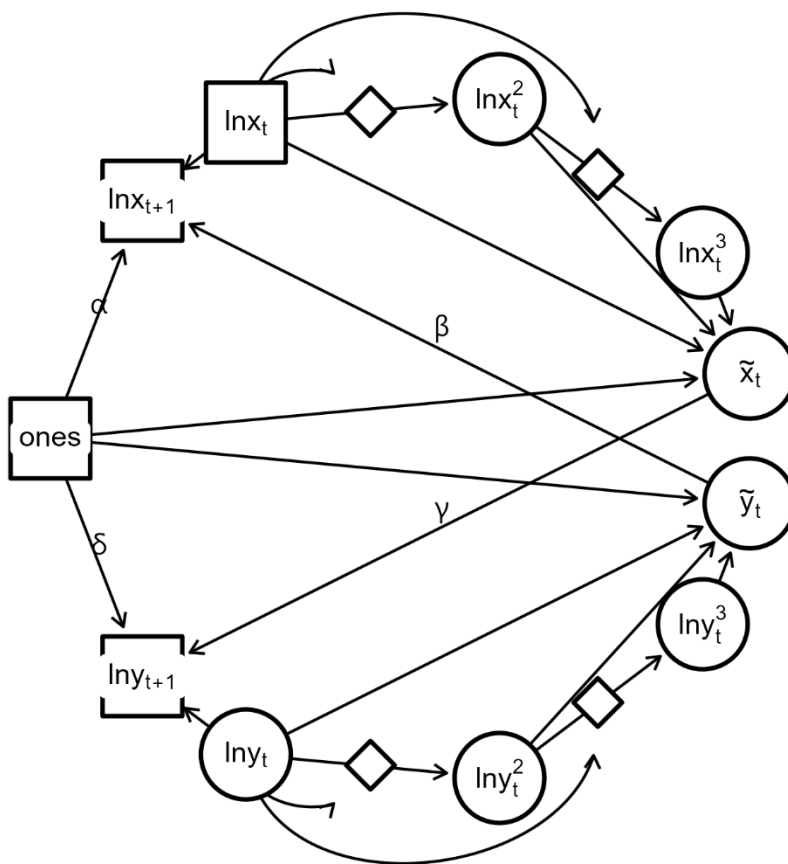
579

580 Table S7: Estimated path coefficients for the Lake Washington case study involving
 581 temperature-dependent resource-consumer-predator dynamics (see Table S4 caption for details)

Path	Lag	Name	Estimate	Std_Error	z_value	p_value
Temp -> Cryptomonas	0	T_to_C	-0.001	0.024	-0.06	0.952
Temp2 -> Cryptomonas	0	T2_to_C	-0.003	0.006	-0.498	0.618
Temp -> Daphnia	0	T_D	0.385	0.074	5.196	0
Temp2 -> Daphnia	0	T2_D	-0.036	0.015	-2.378	0.017
Leptodora -> Daphnia	1	beta	NA	NA	NA	NA
Cryptomonas -> Daphnia	0	alpha	NA	NA	NA	NA
Cryptomonas ->						
Cryptomonas	1	ar_C	0.758	0.038	19.716	0
Daphnia -> Daphnia	1	ar_D	0.577	0.036	16.144	0
Leptodora -> Leptodora	1	ar_L	0.348	0.077	4.533	0
Temp -> Temp2	0	Temp	NA	NA	NA	NA
Temp2 <-> Temp2	0	NA	0.001	NA	NA	NA
alpha <-> alpha	0	NA	0.001	NA	NA	NA
Temp -> alpha	0	T_alpha	0.169	0.044	3.848	0
Temp2 -> alpha	0	T2_alpha	-0.037	0.009	-4.171	0
beta <-> beta	0	NA	0.001	NA	NA	NA
Temp -> beta	0	T_beta	0.003	0.037	0.094	0.925
Temp2 -> beta	0	T2_beta	0.013	0.007	1.809	0.07
Temp <-> Temp	0	V[Temp]	3.825	0.137	27.932	0
Daphnia <-> Daphnia	0	V[Daphnia]	1.218	0.07	17.472	0
Leptodora <-> Leptodora	0	V[Leptodora]	1.373	0.069	19.904	0
Cryptomonas <->						
Cryptomonas	0	V[Cryptomonas]	0.953	0.041	23.043	0

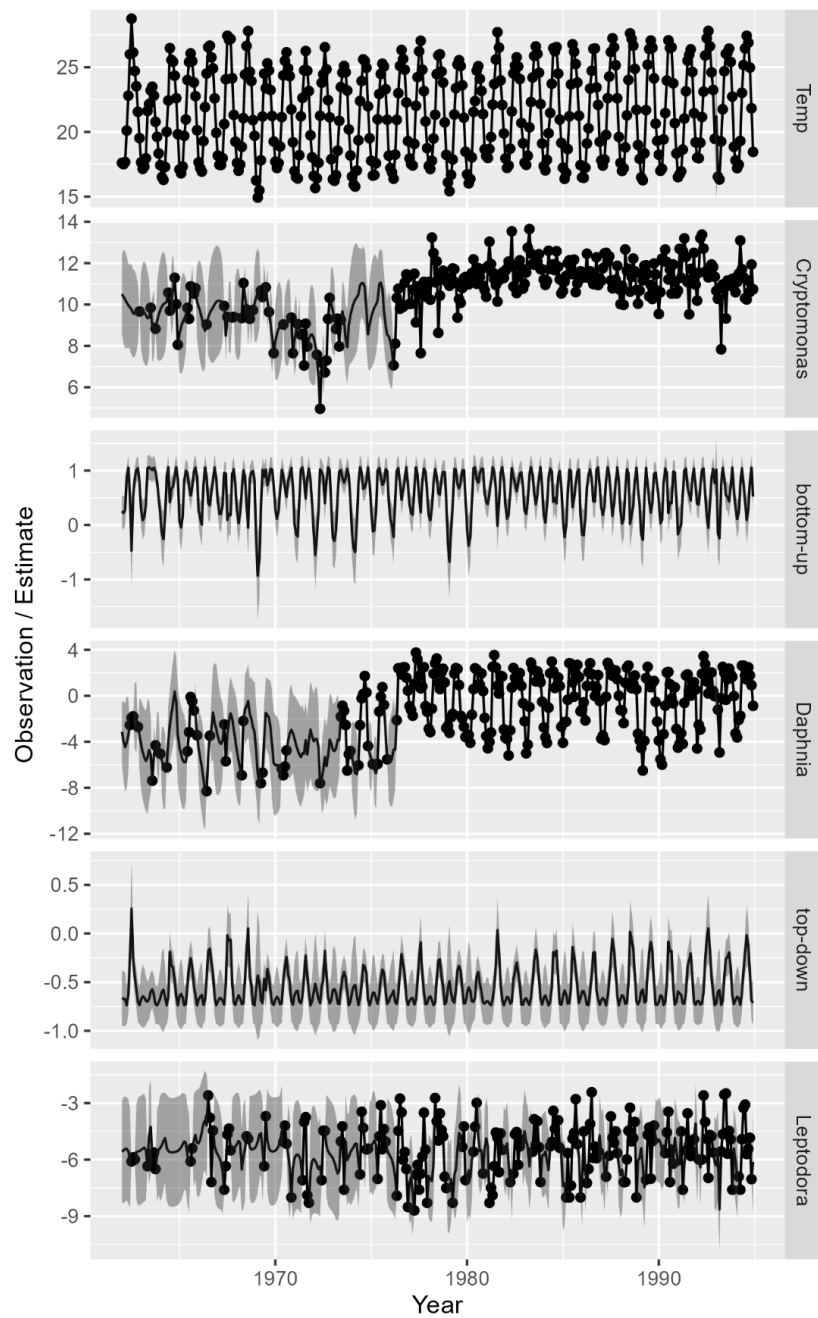
582

583 Fig. S1 -- Graphical model for case study #2 involving Lotka-Volterra predator-prey dynamics
 584 (see Fig. 1 for details about graphical notation), log-abundance for prey $\ln x_t$ and predator $\ln y_t$,
 585 the Taylor-series approximation for abundance \tilde{x}_t and \tilde{y}_t , a vector *ones* representing a model
 586 intercept, and the four estimated interaction parameters ($\alpha, \beta, \gamma, \delta$).



587
 588
 589

590 Fig. S2 – Observed values (circles), estimated values (lines), and 95% confidence intervals
591 (shaded area) for case study #3.



592